Altered ultrastructural morphology of self-aggregated low density lipoproteins: coalescence of lipid domains forming droplets and vesicles

John R. Guyton, Keith F. Klemp, and Martha P. Mims

Departments of Medicine and Cell Biology, Baylor College of Medicine, The Methodist Hospital, Houston, TX 77030

Abstract Lipid droplets and vesicles can presumably be formed directly from lipoproteins in the extracellular space in atherosclerosis, but an in vitro demonstration of the phenomenon in the absence of cellular pathways has been lacking. Low density lipoproteins (LDL) are known to undergo self-aggregation after brief vortexing in vitro. In the present study, LDL aggregates were examined by electron microscopy, using new mordant techniques for lipid visualization, and by chemical analysis. Aggregation of LDL by vortexing is regularly accompanied by the formation of comparatively large lipid droplets (up to 600 nm diameter) and vesicles. Aggregates containing droplets and vesicles were formed after as little as 5 sec of vortexing, and LDL protein and cholesteryl ester were almost completely (95%) incorporated into aggregates after 4 min vortexing. Substantial fractions of phospholipid and unesterified cholesterol from the original LDL remained in solution even after 4 min vortexing, forming large multilamellar vesicles that did not adhere to the aggregated material. Spontaneous aggregates retrieved from LDL solutions after prolonged storage were also examined by electron microscopy, revealing similar lipid droplets and vesicles. ■ The ultrastructural appearance of LDL aggregated in vitro is remarkably similar to the appearance of extracellular lipid deposits in atherosclerosis, lending credence to the hypothesis of direct extracellular formation of these deposits from lipoproteins.—**Guyton, J. R., K. F. Klemp, and M. P. Mims.** Altered ultrastructural morphology of self-aggregated low density lipoproteins: coalescence of lipid domains forming droplets and vesicles. *J. Lipid Res.* 1991. **32:** 953–962.

Supplementary key words electron microscopy • aggregates • cholesteryl ester • cholesterol • phospholipid • multilamellar vesicles • vortexing

The lipid-rich core region found in most human atherosclerotic fibrous plaques contains abundant extracellular lipid deposits that may develop via two general pathways. The first pathway is accumulation of lipoprotein-derived lipid in foam cells, followed by death of the cells. A second general mechanism involves direct formation of lipid droplets and vesicles from normal or altered lipoproteins in the extracellular space. These two pathways are not mutually exclusive; they likely act in concert.

Recent studies have focused attention on the direct extracellular pathway of lipid deposition in atherosclerosis, by finding ultrastructural evidence for this pathway in human and animal arterial specimens (1–5). New mordant techniques, useful for the visualization of lipid deposits by thin-section transmission electron microscopy, were applied to the core region of mature human aortic fibrous plaques, revealing that the predominant lipid ultrastructural forms consisted of small droplets and vesicles (1, 6). The small sizes of extracellular lipid droplets found in the core region favored an origin other than foam cells, which contained much larger lipid droplets. This was in accord with Smith's early suggestion (7) that an extracellular pathway was responsible for most cholesteryl ester deposition in the core region, a suggestion based on the patterns of fatty acyl groups in the esters. Furthermore, evidence suggesting that low density lipoproteins (LDL) may be retained in the arterial intima via binding to extracellular tissue elements has also been reported (8–10).

Conspicuously lacking from studies related to extracellular lipid deposition in atherosclerosis is a demonstration of in vitro formation of lipid droplets and vesicles from LDL particles without cellular uptake and processing. Since the sizes of extracellular lipid deposits (droplets of 30–400 nm diameter, and vesicles somewhat larger) greatly exceed the size of LDL (22 nm diameter), their formation must involve rearrangement of lipid domains and at least partial dissociation of LDL lipids from apolipoprotein B. Neither of these processes has been demonstrated previously to occur in the absence of cellular enzymatic pathways.

Recently Khoo and colleagues (11) described the self-aggregation of LDL subjected to brief vortexing in vitro. LDL aggregates formed in this manner were rapidly in-

---

Abbreviations: LDL, low density lipoproteins; PBS, phosphate-buffered saline.

gested and degraded by macrophages, resulting in an accumulation of neutral lipid within the cells. However, the morphology of the LDL aggregates themselves was not defined.

In the present study, we have examined LDL aggregates by electron microscopy using recently described mordant techniques (6) and chemical analysis. The results suggested that LDL structure was profoundly disrupted by brief vortexing, leading to the formation of lipid droplets and vesicles. Spontaneous aggregates found in LDL after prolonged storage have also been examined, revealing a similar morphology. The process of LDL aggregation may provide a clue to the mechanism of extracellular lipid deposition in atherosclerosis.

METHODS

Materials

Ethylenediamine tetraacetic acid (EDTA) was obtained from Fisher Scientific (Pittsburgh, PA), D-phenylalanyl-L-prolyl-L-arginine chloromethyl ketone (PPACK) from Calbiochem (San Diego, CA), phenylmethylsulfonyl fluoride (PMSF) from Boehringer Mannheim (Indianapolis, IN), butylated hydroxytoluene (BHT) from Sigma (St. Louis, MO), and egg lecithin from Avanti Polar Lipids (Pelham, AL).

Lipoprotein isolation

Fresh human plasma for isolation of LDL was treated with 0.1% EDTA, 1 μM PPACK, 10 μM PMSF, and 20 μM BHT to inhibit proteolysis and lipid oxidation. LDL was isolated by sequential ultracentrifugation between d 1.019 and 1.063 g/ml. Isolated LDL were dialyzed extensively against phosphate-buffered saline (PBS) or against 10 mM diethylmalonic acid, 150 mM NaCl (DEM buffer) at pH 7.4. Both buffers contained 0.01% EDTA.

Vortexing procedure and aggregate separation

Lipoproteins (0.5 mg protein/ml) were pipetted into 12 × 75 mm standard flint glass tubes or polystyrene tubes, 1.2 ml per tube, and vortexed with a Vortex-Genie mixer (American Scientific Products, McGaw Park, IL) for periods from 5 sec to 4 min. As a measure of aggregation, the absorbance of aliquots of vortexed LDL, transferred into individual cuvettes using a Pasteur pipet, was measured at 680 nm using unvortexed LDL as the sample blank.

After the absorbance was measured, the vortexed LDL was transferred to individual 1.5 ml capacity microcentrifuge tubes, using the original pipet, and centrifuged for 10 min at 10,000 g. The supernatant was transferred to a separate microcentrifuge tube and diluted to 1.2 ml with PBS. Meanwhile, 30 μl of a 10% sodium dodecyl sulfate

(SDS) solution and 100 μl of PBS were added to the original flint culture tube used for aggregation. The tube was rinsed vigorously with the SDS-PBS solution and this solution was then transferred, using the same pipet, to the cuvette for further vigorous rinsing to dissolve adhering aggregates. Precipitated material in the microcentrifuge tube was vortexed briefly to disperse it. SDS-PBS solution from the cuvette was transferred to the microcentrifuge tube, and the tube was vortexed vigorously to dissolve the pellet completely. This material was then diluted to 0.5 ml with PBS prior to assay. All vortexing and analytical procedures were performed in duplicate for each experimental condition.

Chemical assays

The total cholesterol content of each sample was determined using a kit supplied by Boehringer Mannheim, which incorporated both cholesteryl esterase and cholesterol oxidase. To provide optimal validation of results, a nationally supplied pooled serum standard was used (Sercal, Center for Disease Control, Atlanta, GA). The content of free cholesterol in each sample was determined in the following manner. An aliquot of the sample was combined with an equal volume of isopropanol and incubated with shaking overnight at 40°C, to assure complete availability of lipids for the assay. An enzymatic cholesterol analysis kit from Boehringer Mannheim, lacking cholesteryl esterase, was then used with free cholesterol (Sigma) dissolved in isopropanol as a standard. To compare the two methods, both were used to assay the cholesterol content of vesicles prepared by sonicating egg lecithin with cholesterol, mixed at a mass ratio of 10:1. On the basis of these assays, performed in conjunction with each experiment, a correction factor ranging from 0.88 to 0.97 was applied to the free cholesterol assay.

Protein concentrations were determined by the assay of Lowry et al. (12), using bovine serum albumin as a standard. In experiments performed with DEM buffer, phosphorus content was assayed by the method of Bartlett with inorganic phosphate as a standard (13). Phospholipid mass was assumed to be 25 times phosphorus mass.

In order to judge the recoveries, the lipid and protein contents of the precipitate and supernatant were summed and compared with the original contents of LDL before vortexing. Recoveries of protein and each lipid class ranged between 95% and 103% in every experiment.

Electron microscopy

For negative staining, unaggregated LDL or small portions of aggregated LDL were stained with 2% uranyl acetate on Formvar-coated copper grids.

For thin-section transmission electron microscopy, native and aggregated LDL samples at a protein concentration of 500 μg/ml were combined with an equal volume of 0.7% OsO$_4$ in PBS or DEM buffer. Native LDL parti-

cles, even after fixation, did not form visible clumps. However, sufficient fixed native LDL could be retained on the surface of a 0.22 μm filter (Millipore GS) to provide material for EM. LDL aggregates and the filters carrying native LDL were embedded in agar and chopped into small pieces for further processing. Specimens were processed by two alternative techniques: the osmium-tannic acid-paraphenylenediamine (TA-PDA) and osmium-thiocarbohydrazide-osmium (OTO) techniques as described previously (6). In the TA-PDA technique, specimens were treated with 1% tannic acid in half-strength buffer for 30 min, followed by a 5-min wash in 1% Na_2SO_4 in half-strength buffer. After three changes of 70% ethanol for 5 min each, the specimens were treated with 1% paraphenylenediamine in 70% ethanol for 30 min. The dehydration schedule was as follows: 70% ethanol 3 × 5 min; 95% ethanol 1 × 15 min, 100% ethanol 3 × 5 min. This was followed by 1:1 ethanol:Epon for 1 h, 100% Epon overnight, Epon for two changes of 2 h each, and embedding in Epon. In the OTO method, specimens were rinsed four times for 3 min each in buffer, then briefly in H_2O, and then treated with 1.5% thiocarbohydrazide for 5 min. This was followed by four changes of buffer for 3 min each, another brief rinse in water, and fixation in 2% buffered OsO_4. Dehydration was as follows: 50% ethanol 1 × 10 min, 70% ethanol 1 × 10 min, 95% ethanol 1 × 15 min, 100% ethanol 3 × 5 min. Infiltration and embedding in epoxy resin were the same as above.

Thin sections of Epon-embedded material were cut on an LKB III Ultrotome. A JEOL 200CX electron microscope was used for ultrastructural observations. The profile diameters of 100 particles of native LDL were measured to assess their size after processing by the TA-PDA technique.

RESULTS

Turbidity

The turbidity of LDL solutions as documented by absorbance at 680 nm increased rapidly with brief vortexing (**Fig. 1**, top panel). Aggregates formed visible clumps, which increased in size as vortexing continued up to 4 min.

Electron microscopy of aggregates after vortexing

Fig. 2 shows the appearance of native LDL and LDL aggregates, as revealed by the TA-PDA mordant technique. Native LDL visualized by this technique had profile diameters of 20.4 ± 2.0 nm (mean ± standard deviation). Micrographs of aggregated LDL always showed numerous droplets of neutral lipid ranging up to 600 nm in profile diameter. A lesser number of lipid vesicles were interspersed with the droplets. Nondescript granular material, within which round shapes consistent with in-

tact LDL particles could be found, occupied spaces adjacent to the larger lipid structures. All of these structural forms were arranged in broad, irregular chains usually 50–200 nm wide. The ultrastructural appearance of aggregated LDL did not vary appreciably with the macroscopic size of aggregates or the time of vortexing. As little as 5 sec of vortexing at low power produced aggregates containing lipid droplets and vesicles. As expected, electron microscopy of OTO-stained material (not shown), did not demonstrate vesicles well (6), but otherwise confirmed the results of TA-PDA-processed material.

Negative stain electron microscopy of LDL aggregated, by vortexing, confirmed the presence of lipid droplets, vesicles, and intact LDL particles (**Fig. 3**). In addition,
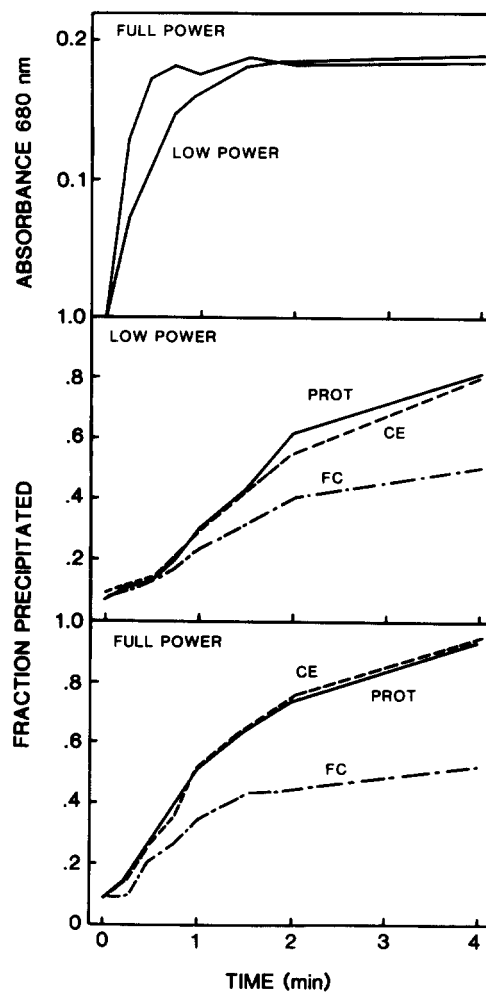

Fig. 1. Time course of LDL aggregation during vortexing of a solution containing LDL at a concentration of 0.5 mg protein/ml. Physical alteration of LDL is shown by changes in absorbance (top panel) and by incorporation of chemical components into precipitable aggregates (bottom two panels). Cholesteryl ester (CE) tends to be incorporated with protein (PROT) into precipitable aggregates, while a substantial portion of free cholesterol (FC) remains in solution in the supernatant even in extensively aggregated specimens. Full power refers to the control setting on a routine test tube vortexing device. Low power is 3/10 of the full power setting.
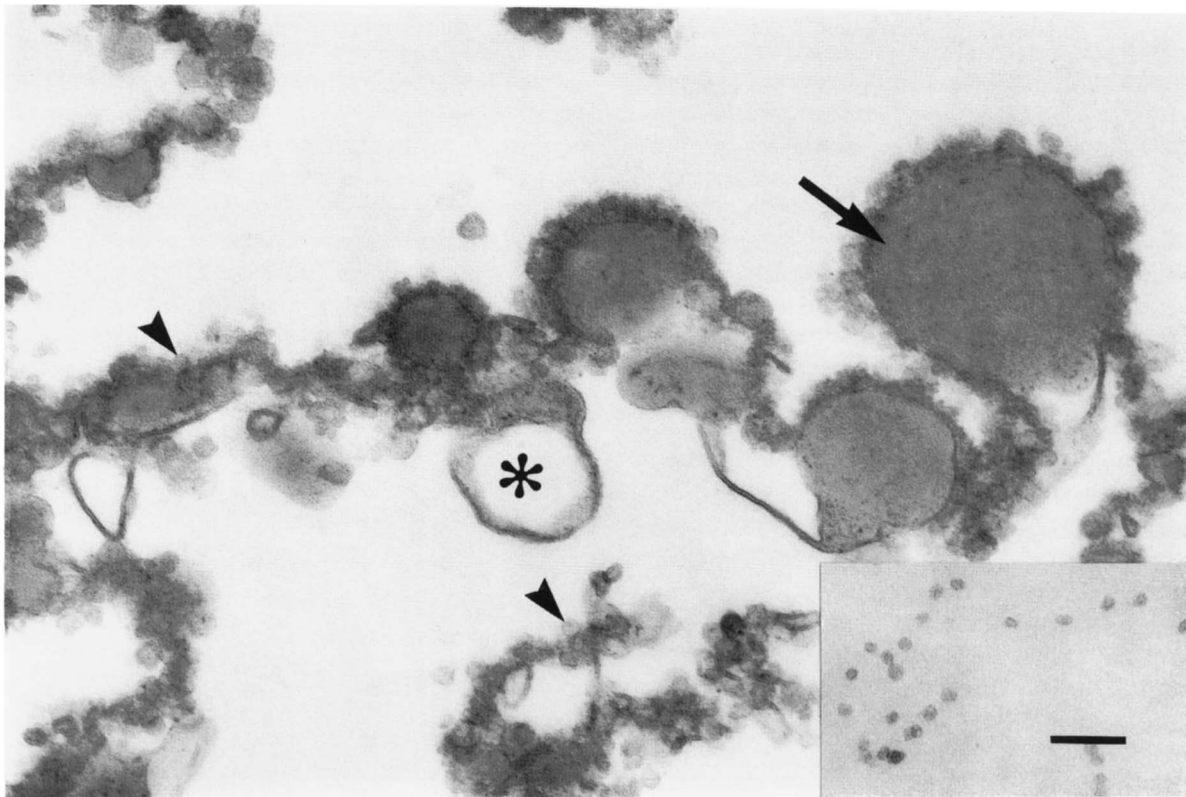
Fig. 2. Ultrastructural appearance of LDL aggregates after vortexing. Lipid droplets of sizes ranging up to 350 nm diameter (arrow) are present along with granular material, particles the size of LDL (arrowheads), and lipid vesicles (asterisk). The aggregated material is arranged in broad strands. Thin-section transmission electron microscropy of material fixed with OsO_4 and stained with tannic acid and paraphenylenediamine (TA-PDA) mordant technique. Inset: native LDL processed similarly. Both figures ×96,000; bar=100 nm.
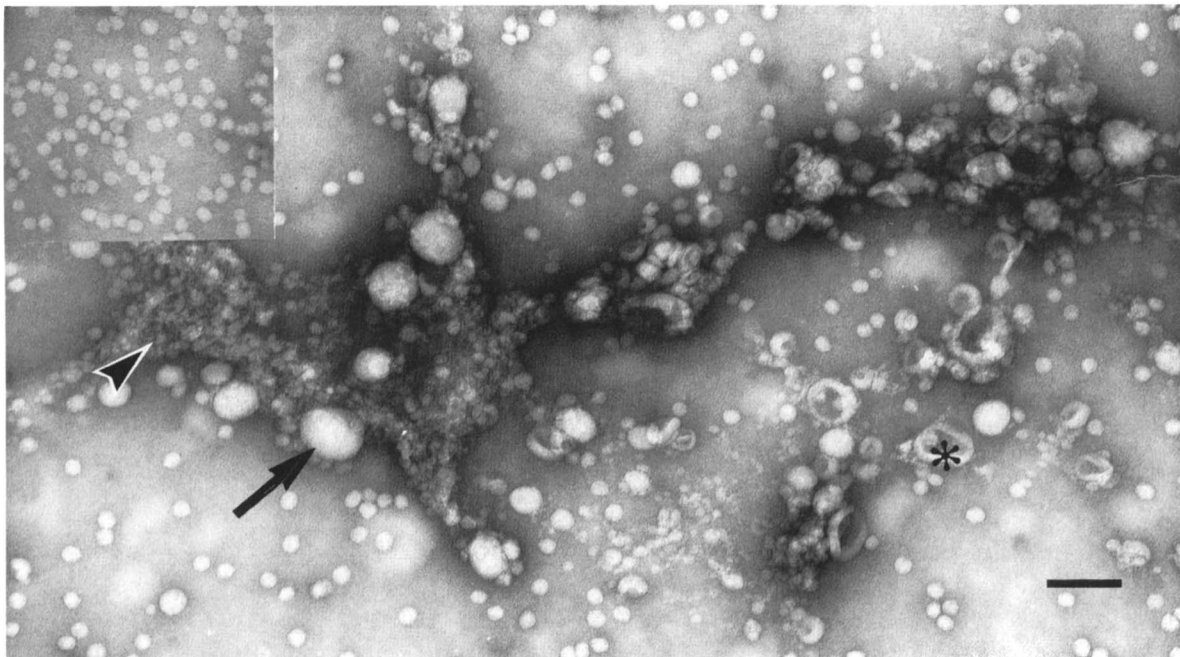

Fig. 3. Negative stain electron microscopy of LDL aggregates. Both lipid droplets (arrow) and vesicles (asterisk) are seen. Normal LDL are found attached to aggregates and unattached. Granular material with particle dimensions less than the size of LDL is seen (arrowhead), suggesting the present of apoB partially dissociated from LDL lipids. Inset: unvortexed LDL. Both figures ×96,000; bar=100 nm.
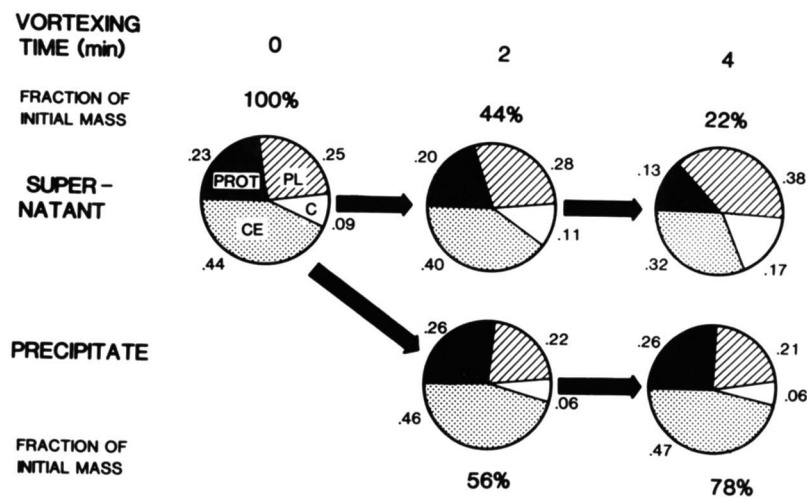
Fig. 4. Analysis of protein content and three major lipid classes in unvortexed LDL (left, time zero) and in precipitable aggregates and soluble supernatant fraction after 2 and 4 min of vortexing; protein (PROT), cholesteryl ester (CE), free cholesterol (C), and phospholipid (PL). Compositions expressed as decimal fractions surround each pie graph. The most marked compositional changes are found in the soluble supernatant fraction after 4 min vortexing. The total lipid + protein masses found in supernatant and precipitate fractions, divided by initial total mass, are designated as fractions of initial mass and expressed as percentages.

areas of granular material with particle sizes much less than that of intact LDL were seen. This material was interpreted as representing denatured apolipoprotein B and remaining associated lipids after disruption of LDL particles.

Chemistry of LDL aggregation

LDL aggregates formed by vortexing were separated from remaining soluble material by brief centrifugation at approximately 10,000 g. The mean fractions of protein
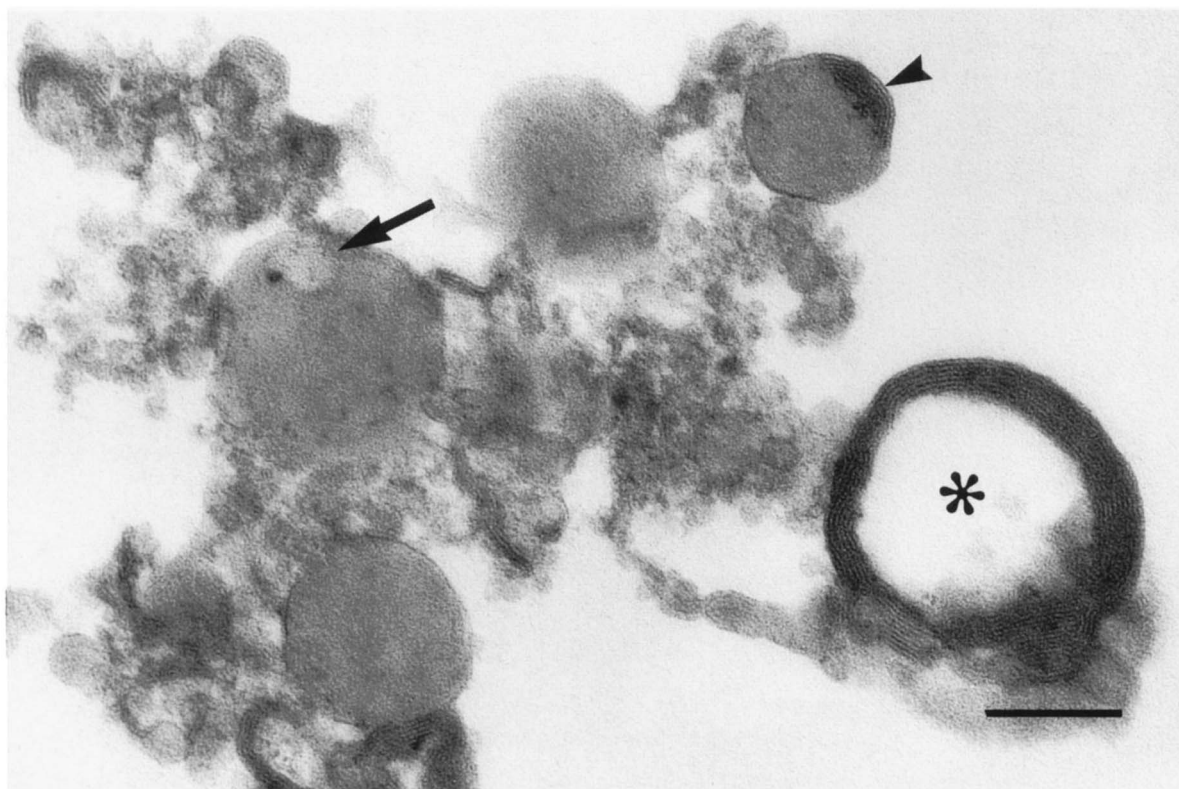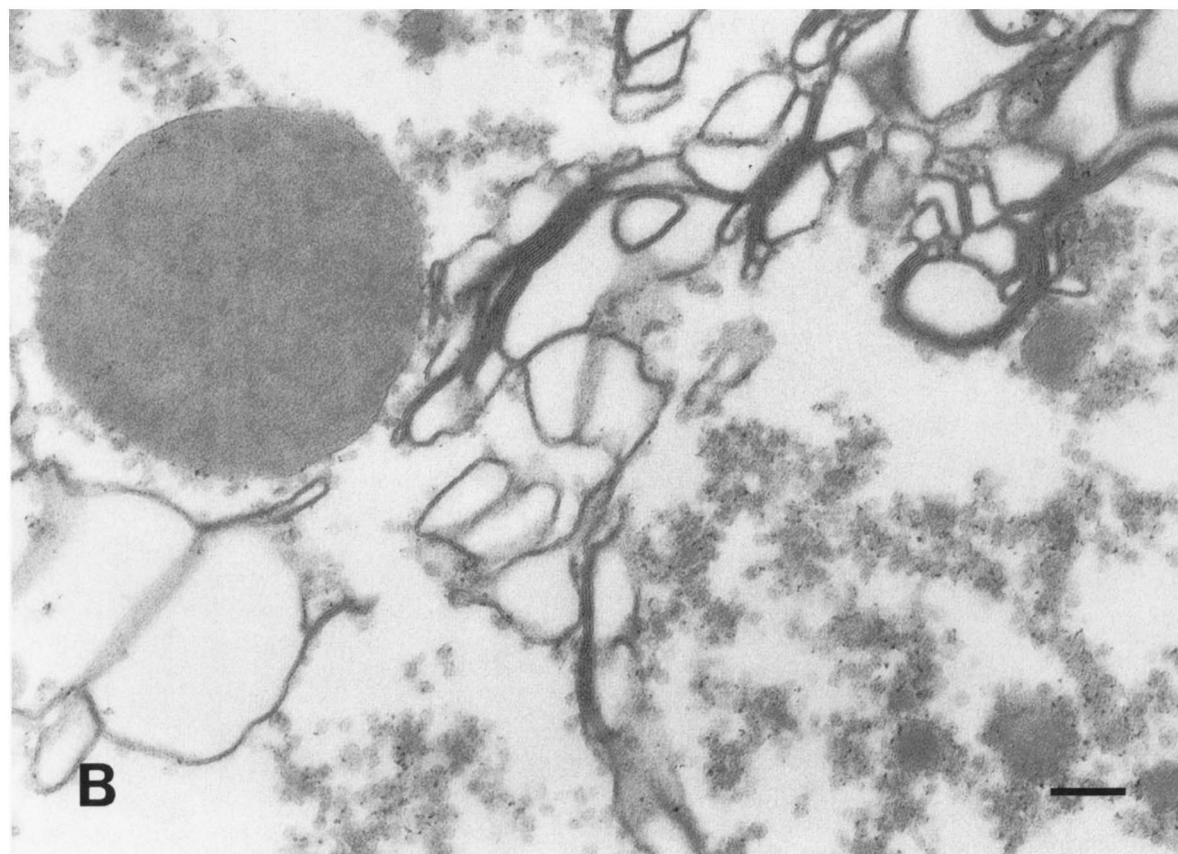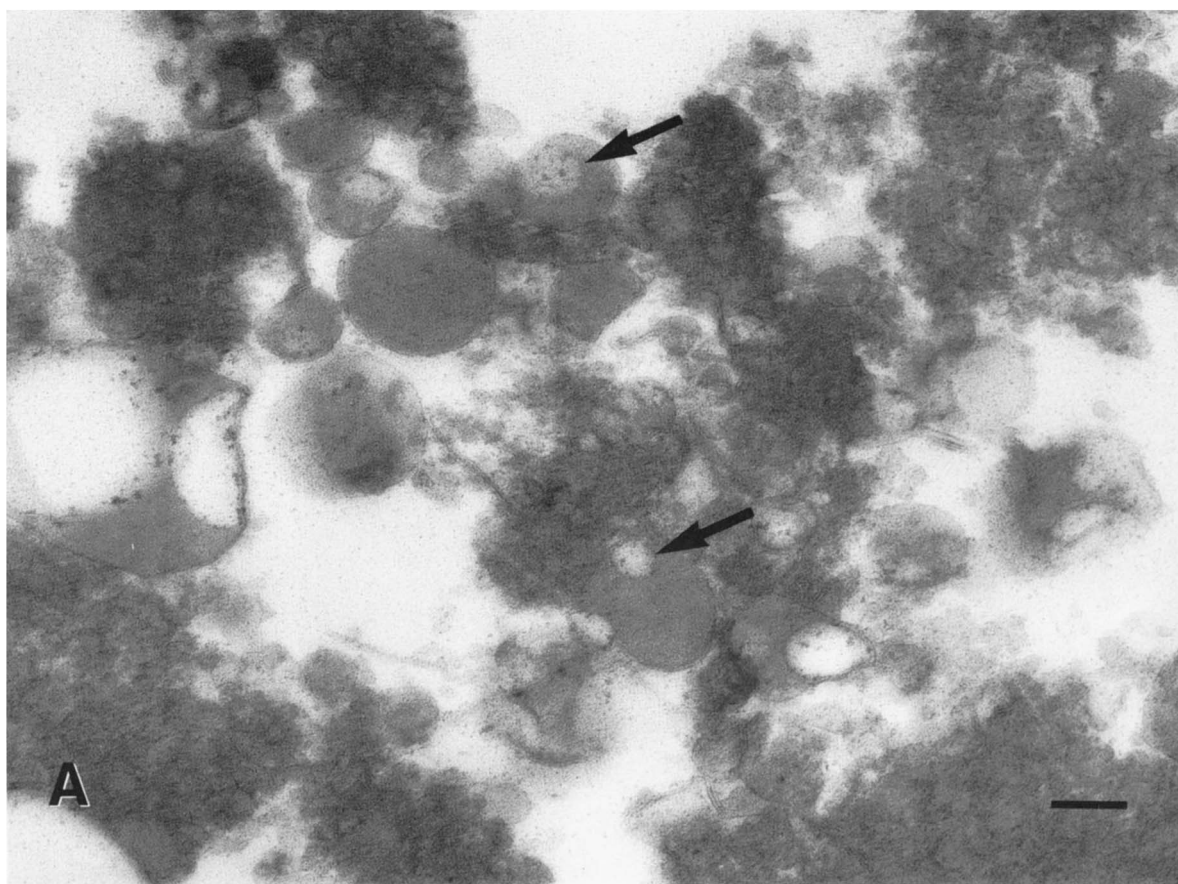

Fig. 5. Ultrastructural appearance of material concentrated from the soluble supernatant fraction after vortexing LDL for 4 min. Lipid droplets, multilamellar vesicles (asterisk), and particles of LDL size are seen. One lipid droplet has a pitted morphology (arrow) and another droplet has a lamellar cap (arrowhead). Thin-section TEM, TA-PDA technique. ×96,000; bar=100 nm.

and lipids incorporated into aggregates and subsequently precipitated by centrifugation are shown in Fig. 1, lower panels. After 4 min vortexing at full power, 95% of protein and cholesteryl ester initially present in the LDL solution were incorporated into aggregates. The fraction of cholesteryl ester incorporated into aggregates closely paralleled the fraction of protein. However, only 59% of free cholesterol was found in aggregates after 4 min. Similar results were obtained for low power vortexing. Fig. 1 also shows that turbidity measurements did not accurately reflect the mass of material incorporated into aggregates, since mass measurements continued to increase well after the development of maximum turbidity.

Fig. 4 shows the results of the analyses of the three major lipid classes in LDL as well as the protein content. One LDL specimen was divided and vortexed in both plastic and flint glass test tubes, in order to test the effect of an altered liquid-solid interface. An LDL specimen from another patient was vortexed in glass test tubes. The three sets of experimental results were all similar; Fig. 4 shows average results. After 4 min, 78% of the total measured lipid-protein mass was incorporated into precipitable aggregates, and 22% remained in solution. Compositional changes were most marked in the supernatant, soluble material after 4 min vortexing. The phospholipid content of this material was 38%, compared to 25% in the original LDL, and the free cholesterol content was 17%, compared to 9% in the original LDL.

Electron microscopy of soluble material after vortexing

The relative increase in phospholipid and free cholesterol content of the soluble fraction suggested that lipid structures other than LDL particles might be present. To visualize these structures, the soluble fraction was concentrated gently by surrounding a dialysis bag with a hygroscopic gel (Aquacide, Calbiochem), and the concentrated material was submitted to electron microscopy. The most prominent lipid structures were multilamellar vesicles, consistent with the presence of excess phospholipid and free cholesterol in the soluble fraction (**Fig. 5**). Lipid droplets and particles resembling intact LDL were also present.

Electron microscopy of spontaneous aggregates

Three small specimens of LDL aggregates that formed spontaneously during storage of LDL at 4°C for 2-3 months were examined. The LDL samples were stored under sterile conditions in 0.9% NaCl, 0.01 M sodium phosphate with 0.01% EDTA, and in 0.9% NaCl with 0.05% EDTA. A limited degree of spontaneous aggregation is common in LDL kept in various buffers for this period of time, in our experience. Electron microscopy revealed lipid droplets and vesicles somewhat similar to those in induced aggregates, but the morphology of the spontaneous aggregates was not as consistent as that of induced aggregates and, in fact, varied considerably among the three specimens (**Fig. 6**). The spontaneous aggregates generally contained larger numbers of apparently intact LDL. Lipid droplets in one spontaneously aggregated specimen showed pits and blebs (Fig. 6A) identical in appearance to those we observed previously in the core region of human atherosclerotic plaques (1).

DISCUSSION

This study has shown that the self-aggregation of LDL that occurs during vortexing and during prolonged storage is accompanied by physical changes in lipoprotein structure leading to the formation of comparatively large lipid droplets and vesicles. The droplets and vesicles are remarkably similar to those demonstrated in previous work to occur in extracellular locations in human arterial specimens (1-3, 6).

The altered structure of LDL aggregates in this study was demonstrated best by new mordant techniques developed for thin-section transmission electron microscopy of lipid deposits in atherosclerosis (6). Negative stain electron microscopy confirmed the presence of droplets and vesicles and additionally revealed granular material suggestive of denatured, partially delipidated apoB. Chemical analysis confirmed the disruption of LDL particles, since aggregates differed in composition from material remaining in solution. Cholesteryl ester tended to be incorporated into aggregates with apoB, while phospholipid and free cholesterol tended to remain in solution. Numerous droplets of neutral lipid observed by electron microscopy within aggregates were consistent with the enrichment of cholesteryl ester in this fraction. A distinct ultrastructural appearance was found in the material remaining in solution, which consisted of multilamellar vesicles as well as some droplets and morphologically normal LDL particles. The presence of numerous vesicles in this fraction was consistent with the marked enrichment of phospholipid and free cholesterol.

Fig. 6. Spontaneous LDL aggregates of variable ultrastructural appearance. A. LDL aggregate withdrawn from LDL stored in saline with 0.05% EDTA. Pitted and blebbed lipid droplets (arrows) are abundant, along with masses of gray material suggesting closely aggregated LDL particles. B. LDL aggregate taken from LDL stored in phosphate-buffered saline with 0.01% EDTA. A large lipid droplet (diameter = 425 nm) is seen at upper left, and several smaller ones are associated with aggregated LDL particles at lower right. Unilamellar and multilamellar vesicles are also seen. Both figures thin-section TEM, TA-PDA technique. ×118,000; bar = 150 nm.

Previous studies of LDL aggregation

Khoo and colleagues (11) first delineated the striking susceptibility of LDL to aggregation by brief vortexing. Our results confirmed the findings of these workers that turbidity increased rapidly in a vortexed LDL solution and that the majority of LDL protein was incorporated into aggregates within 1 to 4 min. Khoo et al. (11) also described the uptake of aggregated LDL into mouse peritoneal macrophages leading to foam cell formation. However, their studies did not examine aggregated LDL by ultrastructural methods.

Treatment of LDL with phospholipase C was shown by Suits et al. (14) to produce aggregates, which were phagocytosed by macrophages via an LDL receptor-dependent mechanism. Transmission electron microscopy performed in their study revealed aggregated particulate material, but extracellular lipid droplets were not described. However, the leaching of neutral lipid by solvents during routine tissue processing for electron microscopy, especially when lipid droplets appear extracellularly, makes it impossible to rule out lipid droplet formation in their study. Neither can one exclude the presence of lipid droplets within the insoluble complexes formed when LDL is mixed with proteoglycans or other extracellular tissue components under varying conditions (8, 15).

Similarity to atherosclerotic lipid deposits

Of particular interest is the resemblance between the lipid droplets and vesicles observed in this study and those found in extracellular locations in human arterial specimens. Of the total area occupied by neutral lipid in the core region of mature fibrous plaques in human aorta, approximately 90% occurred in droplets with profile diameters ranging from 30–400 nm (1). Since cholesteryl ester accounts for the vast majority of neutral lipid in atherosclerosis, one can conclude that the predominant form of cholesteryl ester in the fibrous plaque core region is droplets similar in size to those observed in LDL aggregates. In contrast, foam cell lipid droplets almost always have profile diameters considerably greater than 400 nm (3). Therefore, the small sizes of most extracellular lipid droplets in human atherosclerosis are not consistent with the notion that these droplets are derived from foam cell necrosis, unless an additional and as yet undemonstrated process of disruption of large cellular droplets occurs. But a process related to LDL aggregation might produce small lipid droplets directly in the extracellular space. Furthermore, small extracellular lipid droplets similar in appearance to those demonstrated in this study have also been found in the nascent atherosclerotic core region of fibrolipid lesions (progenitor or early fibrous plaques) and in intimate relationship to elastic and collagenous fibers in nonatherosclerotic human aorta (2, 3).

The lipid droplets found in aggregated LDL preparations were not always spherical; variant morphologies appeared in almost every microscopic field. Occasionally the altered morphology resembled the pitting and blebbing of droplets demonstrated previously in human normal and atherosclerotic arteries (1, 2). In particular, one specimen of spontaneously aggregated LDL had lipid droplets with frequent pitting and blebbing dramatically similar to those found in vivo. We speculated previously that the phenomenon in vivo might result from cholesteryl ester hydrolysis. That possibility seems less likely in view of the present results, since the pits and blebs in the spontaneously aggregated LDL presumably arose in the absence of cholesteryl ester hydrolysis.

The formation of lipid vesicles during LDL aggregation in vitro may help to explain the presence of vesicles in atherosclerotic lesions. Cellular mechanisms for the formation of cholesterol-rich vesicles have been described (16, 17), but the present results suggest the additional possibility of a direct extracellular process. We found that phospholipid and unesterified cholesterol dissociated from LDL during vortexing and formed vesicles. Multilamellar vesicles tended to detach from the aggregated LDL and to remain in the supernatant fraction after precipitation of the aggregates by centrifugation. This fraction was enriched in phospholipid and unesterified cholesterol. Scattered unilamellar vesicles remained attached to the aggregated LDL and droplets. The production of multilamellar vesicles was especially interesting, since very similar structures are found in extracellular lipid deposits in human atherosclerosis (1). Kruth (18, 19) used filipin staining and fluorescence microscopy to describe particles rich in unesterified cholesterol commonly found in a variety of human and animal atherosclerotic lesions. Isolation of the particles revealed that they were unilamellar and multilamellar vesicles composed predominantly of unesterified cholesterol and phospholipid. Some of the particles also contained a significant amount of esterified cholesterol, comparable to the hybrid lipid droplet-vesicle structures that we observed in the present study.

Extracellular lipid deposition

By providing an in vitro model for the formation of lipid droplets and vesicles from LDL in the absence of cells, the present results bolster the hypothesis of direct extracellular deposition of lipid in atherosclerosis. This hypothesis was proposed 20 years ago by Smith (7) on the basis of light microscopic observations of early "perifibrous" lipid deposition associated with elastic and collagen fibers and detailed studies of the cholesteryl ester fatty acyl patterns in atherosclerotic lesions. The early light microscopic description of perifibrous lipid has been amplified by a recent ultrastructural study, which showed that deposits of neutral lipid are often found within the interstices of elastic fibers, a location inconsistent with direct

derivation from necrotic foam cells (2). Smith (7) found cholesteryl ester in the core region of fibrous plaques to be rich in cholesteryl linoleate, differing from the cholesteryl oleate-rich pattern found in early foam cell lesions. The cholesteryl ester fatty acyl pattern in the fibrous plaque core region was actually close to that found in plasma lipoproteins, suggesting a direct pathway of lipid droplet formation.

Ultrastructural evidence for lipoprotein aggregation and coalescence of lipid domains occurring in vivo was reported recently by Frank and Fogelman (4). Based on the work of previous investigators, which showed that extracellular lipid deposition was prominent in early rabbit atherogenesis (5, 20), these authors used freeze-etching electron microscopy to examine the aortic intima from Watanabe Heritable Hyperlipidemic (WHHL) rabbits and cholesterol-fed rabbits. They demonstrated round lipid particles ranging in size from 23 to 169 nm enmeshed in the extracellular matrix. The particles commonly appeared in clusters, and within the clusters many particles had the appearance of fusing with each other. Since freeze-etching electron microscopy does not always distinguish lipid droplets from vesicles, the particles observed by Frank and Fogelman (4) probably comprised both types of lipid deposits. Nevertheless, their observations suggest strongly that the processes of lipoprotein aggregation and lipid coalescence demonstrated in vitro in the present study may also occur in vivo.

While our results suggest that extracellular lipid deposition might occur by a process akin to LDL aggregation by vortexing in vivo, it remains to be shown exactly what stimulus might be responsible for LDL aggregation in the arterial wall. Furthermore, the mechanisms of lipid phase rearrangement in vortexed LDL and in the arterial wall remain unknown. Arterial tissue is mechanically active, but the gas–liquid interface presumed responsible for protein denaturation in some systems is obviously absent. Hydrolysis of cholesteryl ester (21), phospholipid (14), or triglycerides (22) and complexation with proteoglycans or other extracellular tissue components (8, 15, 23) have been observed to cause LDL aggregation in vitro. The ultrastructural morphology of such complexes is unknown. As confirmed in the present study, simple storage of LDL is associated with some formation of aggregates, which possess a variable morphology of lipid droplets and vesicles similar to aggregates produced by vortexing. Recently it has been suggested that the process of aggregate formation may be accelerated in LDL modified by oxidation, glycosylation, desialylation, and treatment with malondialdehyde or 4-hydroxynonenal (24, 25). All of these are candidate stimuli for a process which seems likely to occur in the arterial intima, producing extracellular lipid deposits. ▐▌

REFERENCES

1. Guyton, J. R., and K. F. Klemp. 1989. The lipid-rich core region of human atherosclerotic fibrous plaques: prevalence of small lipid droplets and vesicles by electron microscopy. *Am. J. Pathol.* **134:** 705–717.
2. Guyton, J. R., T. M. Bocan, and T. A. Schifani. 1985. Quantitative ultrastructural analysis of perifibrous lipid and its association with elastin in nonatherosclerotic human aorta. *Arteriosclerosis.* **5:** 644–652.
3. Bocan, T. M., T. A. Schifani, and J. R. Guyton. 1986. Ultrastructure of the human aortic fibrolipid lesion. Formation of the atherosclerotic lipid-rich core. *Am. J. Pathol.* **123,** 413–424.
4. Frank, J. S., and A. M. Fogelman. 1989. Ultrastructure of the intima in WHHL and cholesterol-fed rabbit aortas prepared by ultra-rapid freezing and freeze-etching. *J. Lipid Res.* **30:** 967–978.
5. Simionescu, N., E. Vasile, F. Lupu, G. Popescu, and M. Simionescu. 1985. Prelesional events in atherogenesis: accumulation of extracellular cholesterol-rich liposomes in the arterial intima and cardiac valves of the hyperlipidemic rabbit. *Am. J. Pathol.* **123:** 109–125.
6. Guyton, J. R., and K. F. Klemp. 1988. Ultrastructural discrimination of lipid droplets and vesicles in atherosclerosis: value of osmium-thiocarbohydrazide-osmium and tannic acid-paraphenylenediamine techniques. *J. Histochem. Cytochem.* **36:** 1319–1328.
7. Smith, E. B. 1974. The relationship between plasma and tissue lipids in human atherosclerosis. *Adv. Lipid Res.* **12:** 1–49.
8. Camejo, G. 1982. The interaction of lipids and lipoproteins with the intercellular matrix of arterial tissue: its possible role in atherogenesis. *Adv. Lipid Res.* **19:** 1–53.
9. Podet, E. J., D. R. Shaffer, S. H. Gianturco, W. A. Bradley, C. Y. Yang, and J. R. Guyton. 1991. Interaction of low density lipoproteins with human aortic elastin. *Arterioscler. Thromb.* **11:** 116–122.
10. Vijayagopal, P., S. R. Srinivasan, B. Radhakrishnamurthy, and G. S. Berenson. 1981. Interaction of serum lipoproteins and a proteoglycan from bovine aorta. *J. Biol. Chem.* **256:** 8234–8241.
11. Khoo, J. C., E. Miller, P. McLoughlin, and D. Steinberg. 1988. Enhanced macrophage uptake of low density lipoprotein after self-aggregation. *Arteriosclerosis.* **8:** 348–358.
12. Lowry, O. H., N. J. Rosebrough, A. L. Farr, and R. J. Randall. 1951. Protein measurement with the Folin phenol reagent. *J. Biol. Chem.* **193:** 265–275.
13. Bartlett, G. R. 1959. Phosphorous assay in column chromatography. *J. Biol. Chem.* **234:** 466–468.
14. Suits, A. G., A. Chait, M. Aviram, and J. W. Heinecke. 1989. Phagocytosis of aggregated lipoprotein by macro-

phages: low density lipoprotein receptor-dependent foam-cell formation. *Proc. Natl. Acad. Sci. USA.* **86:** 2713-2717.

15. Falcone, D. J., and B. G. J. Salisbury. 1988. Fibronectin stimulates macrophage uptake of low density lipoprotein-heparin-collagen complexes. *Arteriosclerosis.* **8:** 263-273.

16. Schmitz, G., H. Robenek, M. Beuck, R. Krause, and R. Niemann. 1988. Ca⁺⁺ antagonists and ACAT inhibitors promote cholesterol efflux from macrophages by different mechanisms. I. Characterization of cellular lipid metabolism. *Arteriosclerosis.* **8:** 46-46.

17. Robenek, H., and G. Schmitz. 1988. Ca⁺⁺ antagonists and ACAT inhibitors promote cholesterol efflux from macrophages by different mechanisms. II. Characterization of intracellular morphologic changes. *Arteriosclerosis.* **8:** 57-67.

18. Kruth, H. S. 1984. Localization of unesterified cholesterol in human atherosclerotic lesions: demonstration of filipin-positive, Oil-Red-O-negative particles. *Am. J. Pathol.* **114:** 201-208.

19. Kruth, H. S. 1984. Filipin-positive, Oil Red O-negative particles in atherosclerotic lesions induced by cholesterol feeding. *Lab. Invest.* **50:** 87-93.

20. Kruth, H. S. 1985. Subendothelial accumulation of unesterified cholesterol. An early event in atherosclerotic lesion development. *Arteriosclerosis.* **57:** 337-341.

21. Chao, F., L. M. Amende, E. J. Blanchette-Mackie, S. I. Skarlatos, W. Gamble, J. H. Resau, W. T. Mergner, and H. S. Kruth. 1988. Unesterified cholesterol-rich lipid particles in atherosclerotic lesions of human and rabbit aortas. *Am. J. Pathol.* **131:** 73-83.

22. Musliner, T. A., K. M. McVicker, J. F. Iosefa, and R. M. Krauss. 1987. Lipolysis products promote the formation of complexes of very-low-density and low-density lipoproteins. *Biochim. Biophys. Acta.* **919:** 97-110.

23. Falcone, D. J., N. Mateo, H. Shio, C. R. Minick, and S. D. Fowler. 1984. Lipoprotein-heparin-fibronectin-denatured collagen complexes enhance cholesteryl ester accumulation in macrophages. *J. Cell. Biol.* **99:** 1266-1274.

24. Tertov, V. V., I. A. Sobenin, Z. A. Gabbasov, E. G. Popov, and A. N. Orekhov. 1989. Lipoprotein aggregation as an essential condition of intracellular lipid accumulation caused by modified low density lipoproteins. *Biochem. Biophys. Res. Commun.* **163:** 489-494.

25. Hoff, H. F., J. O'Neil, G. M. Chisolm III, T. B. Cole, O. Quehenberger, H. Esterbauer, and G. Jurgens. 1989. Modification of low density lipoprotein with 4-hydroxy-nonenal induces uptake by macrophages. *Arteriosclerosis.* **9:** 538-549.